

# Cobalt Protoporphyrin Accelerates TFEB Activation and Lysosome Reformation during LPS-Induced Septic Insults in the Rat Heart

Kana Unuma<sup>1</sup>, Toshihiko Aki<sup>1\*</sup>, Takeshi Funakoshi<sup>1</sup>, Ken-ichi Yoshida<sup>2</sup>, Koichi Uemura<sup>1</sup>

**1** Section of Forensic Medicine, Graduate School of Medical and Dental Sciences, Tokyo Medical and Dental University, Tokyo Japan, **2** Department of Forensic Medicine, Graduate School of Medicine and Faculty of Medicine, University of Tokyo, Tokyo, Japan

## Abstract

Lipopolysaccharide (LPS)-induced myocardial dysfunction is caused, at least in part, by mitochondrial dysfunction. Mitochondrial dysfunction and the oxidative damage associated with it are scavenged through various cellular defense systems such as autophagy to prevent harmful effects. Our recent study has demonstrated that cobalt protoporphyrin IX (CoPPIX), a potent inducer of heme oxygenase-1 (HO-1), ameliorates septic liver injuries by enhancing mitochondrial autophagy in rats. In our current study, we show that CoPPIX (5 mg/kg s.c.) not only accelerates the autophagic response but also promotes lysosome reformation in the rat heart treated with LPS (15 mg/kg i.p.). Lysosomal membrane-associated protein-2 (LAMP2), which is essential to the maintenance of lysosomal functions in the heart, is depleted transiently but restored rapidly during LPS administration in the rat. Activation of transcription factor EB (TFEB), a master regulator of lysosomal biogenesis and autophagy, was also observed, indicating a hyper consumption and subsequent reformation of the lysosome to meet the increased demand for autophagosome cleaning. CoPPIX was found to promote these processes and tended to restore the LPS-induced suppression of cardiac performances whilst chloroquine (CQ; 20 mg/kg i.p.), an inhibitor of lysosomes and autophagic protein degradation, abrogates these beneficial effects. The cardioprotective effect of CoPPIX against LPS toxicity was also observed via decreased levels of cardiac releasing enzymes in the plasma. Taken together, our current data indicate that lysosome reformation mediated by TFEB may be involved in cardioprotection against LPS-induced septic insults, and serve as a novel mechanism by which CoPPIX protects the heart against oxidative stress.

**Citation:** Unuma K, Aki T, Funakoshi T, Yoshida K-i, Uemura K (2013) Cobalt Protoporphyrin Accelerates TFEB Activation and Lysosome Reformation during LPS-Induced Septic Insults in the Rat Heart. PLoS ONE 8(2): e56526. doi:10.1371/journal.pone.0056526

**Editor:** Ramani Ramchandran, Medical College of Wisconsin, United States of America

**Received:** October 30, 2012; **Accepted:** January 10, 2013; **Published:** February 15, 2013

**Copyright:** © 2013 Unuma et al. This is an open-access article distributed under the terms of the Creative Commons Attribution License, which permits unrestricted use, distribution, and reproduction in any medium, provided the original author and source are credited.

**Funding:** This work was supported in part by Grant-in Aid from the Japan Society for the Promotion of Science (Grant 24790639 to K. Unuma, Grant 22590629 to TA and Grant 30586425 to K. Uemura). The funders had no role in study design, data collection and analysis, decision to publish, or preparation of the manuscript.

**Competing Interests:** The authors have declared that no competing interests exist.

\* E-mail: aki.legm@tmd.ac.jp

## Introduction

Lipopolysaccharide (LPS), a major outer cell wall component of gram-negative bacteria, causes septic shock in humans and animals [1]. The administration of LPS to laboratory animals ultimately leads to multi-organ dysfunction that includes myocardial depression [2,3,4]. Cardiac dysfunction is caused by the production of proinflammatory cytokines, mitochondrial dysfunction, and subsequent contractile failure followed by a precipitous drop in cardiac output [2,3,5]. Dysfunctional mitochondria are scavenged to prevent harmful effects including apoptosis induction as well as the generation of reactive oxygen species (ROS). Autophagy has been shown to play pivotal roles in the elimination of dysfunctional mitochondria [6]. Following their elimination, dysfunctional mitochondria should be replaced to ensure that normal cellular functions are not affected. Mitochondrial reformation is mediated by transcription factors/co-factors such as nuclear respiratory factor 1 (NRF1), peroxisome proliferator-activated receptor  $\gamma$  coactivator-1 $\alpha$  (PGC-1 $\alpha$ ), and mitochondrial transcription factor A (TFAM) [7,8]. Indeed, transient mitochondrial depletion followed by regeneration by these factors has been

demonstrated in the hearts of LPS-treated animals as well as in cultured cardiomyocytes [9,10,11].

In addition to the elimination of mitochondria damaged upon pathologic insults, autophagy activation sometimes causes hyper consumption of lysosome to meet with the increased demand for cleaning the autophagosome. This would be resulted in the disturbance of lysosomal degradation and should be repaired by *de novo* synthesis of lysosomes. Yu et al. have shown previously that primary lysosomes are lost during starvation through the formation of secondary autolysosomes and are reformed to their original number after a prolonged starvation period [12]. Although the correct reformation of lysosomes may sometimes be necessary for the completion of cytoprotective autophagy processes, a sub optimal level of lysosome activity and function and subsequent impairment of autophagic flux has been reported in the pathogenesis of various disease models such as Parkinson's disease [13] and pancreatitis [14]. Transcription factor EB (TFEB) is a master regulator of lysosome biogenesis [15] and is also involved in autophagy induction [16]. Lysosome reformation through the actions of TFEB has been shown to block the pathological accumulation of autophagosomes in the brain tissue

of a Parkinson's disease model animal [13]. The forced expression of TFEB also mitigates the cardiomyocyte death caused by the overexpression of pro-apoptotic BNIP3 by enhancing lysosome reformation and the subsequent resumption of the autophagic flux [17].

Heme oxygenase (HO), the rate-limiting enzyme in the heme-degradation pathway, confers cytoprotection against cellular injuries in various tissues and in various models of disease including sepsis [18]. The cytoprotective effects of HO are attributed not only to the breakdown of cytotoxic free heme but also to its catalytic products carbon monoxide (CO) and biliverdin, both of which act as antioxidants [18]. Metalloprotoporphyrins, such as cobalt protoporphyrin IX (CoPPIX), zinc protoporphyrin IX (ZnPPIX), and tin protoporphyrin IX (SnPPIX), are powerful modulators of HO activities [19]. Whilst ZnPPIX and SnPPIX are HO antagonists, CoPPIX works as an inducer of HO-1, an inducible isoform of HO. Recently, we and other groups showed that the pharmacological modulation of HO affects cytoprotective autophagy during LPS administration in the liver: the HO-1 inducer CoPPIX enhances cytoprotective autophagy in the LPS-treated rat liver [20] whilst the HO antagonist SnPPIX suppresses this pathway in CLP/LPS-treated mouse liver/hepatocytes [21].

In our present study, we examined the effects of CoPPIX on the status of the mitochondria, autophagic response, and the lysosome in LPS-treated rat hearts. As observed previously in the LPS-treated rat liver [20], mitochondrial autophagy appeared to take place in the rat heart under LPS exposure. We also observed that LAMP2, an essential molecule for lysosomal functions in the heart [22], is transiently depleted during LPS administration. TFEB and the transcription of LAMP2 are activated in tandem with lysosomal depletion, suggesting that they represent a compensatory mechanism for lysosome depletion during LPS administration. The pharmacological induction of HO-1 by CoPPIX accelerates these phenomena and tends to improve the cardiac performance that has been compromised by LPS.

## Materials and Methods

### Animal experiments

The animal experimentation protocols used in this study were approved by the Institutional Animal Care and Use Committee of University of Tokyo. Five-week-old male Sprague-Dawley rats were injected intraperitoneally (i.p.) with 15 mg/kg LPS [from *Escherichia coli* (*E. coli*) obtained from Sigma (L-2630, St. Louis, MO)] dissolved in 0.5 mL isotonic NaCl, or vehicle ( $n = 4/\text{group}$ ). To determine if the heart damage induced by LPS administration is attenuated by HO-1, an inducer of this enzyme, cobalt protoporphyrin IX [CoPPIX (Sigma), 5 mg/kg in 0.5 mL dimethyl sulfoxide], was injected subcutaneously into the rats 24 h before LPS treatments. Chloroquine (Wako, 20 mg/kg) or tin protoporphyrin IX [SnPPIX (Sigma), 50 mg/kg] was also injected i.p. in some experiments one or 24 h before LPS treatment, respectively. The animals in the control group received vehicle injections at the same time ( $n = 4/\text{group}$ ).

### Transmission electron microscopy

The animals were anesthetized with sodium pentobarbital (Nembutal, Abbott Laboratories, North Chicago, IL) at 60 mg/kg i.p. three hours after LPS injection (15 mg/kg), and then perfused transcardially with saline, followed by treatment with a fixative solution containing 4% paraformaldehyde and 2% glutaraldehyde in 0.1 M phosphate buffer (PB), pH 7.4. After perfusion, the left ventricle of the heart was removed and sliced. After rinsing in 0.2 M PB and post-fixation with buffered 2% osmium tetroxide

for 2 h, the slices were stained en bloc with saturated aqueous uranyl acetate solution for 15 min, dehydrated in a graded ethanol series, and embedded in Epon 812. Ultrathin (90 nm) sections were double stained with uranyl acetate and lead citrate and then examined by transmission electron microscopy (H-7100; Hitachi, Hitachinaka, Japan).

### Western Blotting

Samples were lysed in a buffer containing 10 mM Tris-HCl (pH 8.0), 320 mM sucrose, 1 mM EDTA, protease inhibitor cocktail (Complete, Roche, Mannheim, Germany), and phosphatase inhibitor cocktail (PhosSTOP, Roche). Protein concentrations of the sample extracts were determined using a Coomassie Protein Assay Kit (Thermo Fisher Scientific, Rockford, IL). Five  $\mu\text{g}$  of protein per lane was subjected to SDS-PAGE gels and then electrophoretically transferred to a PVDF membrane (Immobilon-P transfer membrane; Millipore, Billerica, MA). Western blot analysis was performed using the following antibodies: anti-microtubule-associated protein light chain 3 (LC3) (#4445, Cell Signaling Technology, Beverly, MA; 1:5000 dilution), anti-p62/SQSTM1 (#5114, Cell Signaling Technology), anti-nuclear respiratory factor 1 (NRF1) (sc-33771, Santa Cruz Biotechnology, Santa Cruz, CA), anti-mitochondrial transcription factor A (TFAM) (sc-23588, Santa Cruz Biotechnology), anti-transcription factor EB (TFEB) (ab56330, Abcam, Cambridge, MA), anti-lysosome-associated membrane protein 1 (LAMP1) (#3243, Cell Signaling Technology), anti-lysosome-associated membrane protein 2 (LAMP2) (ab37024, Abcam), anti-GAPDH (Millipore, Billerica, MA), and anti-actin (Sigma-Aldrich, St. Louis, MO; 1:5000 dilution). Peroxidase-conjugated anti-rabbit, anti-mouse, or anti-goat IgG antibodies were obtained from Promega (Madison, WI). The target protein levels were determined from a standard curve constructed by plotting the band densities and were normalized to the actin or GAPDH levels using CS Analyzer software, ver. 3.0 (ATTO, Tokyo, Japan).

### Quantitative RT-PCR

Total RNA was prepared from rat heart using TRIzol reagent (Invitrogen, Carlsbad, CA) and reverse transcription was performed using SuperScript II reverse transcriptase (Invitrogen). Quantitative PCR was performed with a StepOnePlus Real-Time PCR System (Applied Biosystems, Foster City, CA) using SYBR green as fluorescence dye. The PCR conditions were as follows: 95°C for 20 s followed by 40 cycles of 95°C for 3 s and 60°C for 30 s. The primers used were: 5'-GCAAGGCGCTCGCCCTCAAT-3' and 5'-GCCCCGGTGACTCCTCTTCC-3' for LAMP1; 5'-AGCAGGTGGTTCCGTGTCTCG-3' and 5'-AGGGCTGCTCCACCGCTAT-3' for LAMP2; and 5'-CACCCGCGAGTACAACCTTCTTG-3' and 5'-CCTCTCTTGCTCTGGGCCTCGT-3' for actin.

### Immunohistochemical staining for anti-transcription factor EB (TFEB) and 4-hydroxy-2-nonenal (4-HNE)

Formalin-fixed, paraffin-embedded sections of rat hearts were subjected to immunohistochemical analysis for TFEB and 4-HNE as previously described. Briefly, the 3- $\mu\text{m}$  thick tissue sections were deparaffinized and rehydrated, followed by microwave retrieval, according to standard procedures. The slides were sequentially blocked with avidin and biotin, and then incubated 4°C overnight with 1/100 diluted mouse anti-4-HNE antibody (Japan Institute for the Control of Aging, Nikken Seil Co., Ltd, Shizuoka, Japan). Following repeat washes, the slides were incubated at 25°C for 30 minutes with biotinylated goat anti-mouse IgG (414241, 1/200

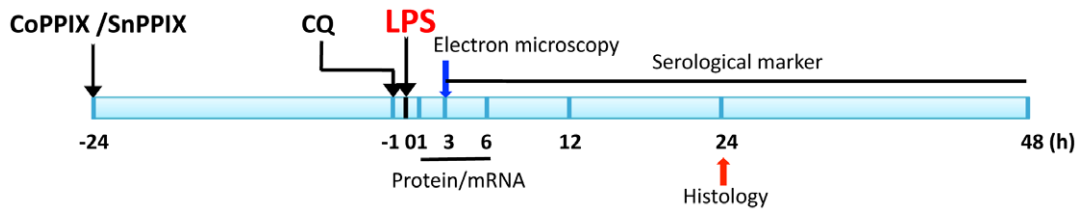


**Figure 1. Time line illustrating the experimental design.**

doi:10.1371/journal.pone.0056526.g001

dilution; Nichirei Biosciences, Tokyo, Japan). Diaminobenzidine (DAB) was used as a substrate, and the slides were dehydrated and covered in DePex. As negative controls, control sections were incubated with mouse IgG instead of the primary antibodies at the same IgG concentrations. The slides were then analyzed under a light microscope (Olympus AX80).

### Hematoxylin and eosin (H&E) staining

The left ventricle hearts and left upper lobe of rat treated with or without LPS and/or CoPPIX were transversely cut at a 2 mm thickness, and immediately fixed in 4% paraformaldehyde and embedded in paraffin. Sections of 3- $\mu$ m thickness were affixed to slides, deparaffinized, and stained with H&E to evaluate morphologic changes.

### Blood analysis

Blood samples (0.2 ml each, anticoagulant in syringe: K3-EDTA at 1.5 mg/ml) were taken from the caudal veins of the rats at 0, 3, 6, 12, 24, and 48 h after LPS injections (15 mg/kg) with or

without CoPPIX treatment. The plasma aspartate aminotransferase (AST) and creatine kinase-MB (CK-MB) levels were then measured using the standard methods of SRL Inc. (Tokyo, Japan).

### Echocardiography

Rats were placed on a warm blanket, and echocardiographic parasternal long-axis images as well as M-mode tracings were obtained at the level of the papillary muscles (famo-v, model SSA-510V, Toshiba, Japan). Measurements from the long-axis views included LV dimensions at end diastole and end systole and fractional shortening. These echocardiographic measurements were made at baseline (preinjection) and at 3 and 24 h after the injection of LPS, CoPPIX, or CQ (n = 4).

### Statistical Analysis

Data are expressed as the means  $\pm$  S.E. Two groups were compared using the Student's t-test. Multiple group comparisons were made using analysis of variance (ANOVA) in combination with the Tukey's or Dunnett post hoc test. For nonparametric statistical analysis, the Kruskal-Wallis test and Steel procedure were used to evaluate the differences between two groups. Differences were considered significant at  $P < 0.05$ .

## Results

### Cytoplasmic vacuolization and mitochondrial damage during LPS-administration in the heart

Experimental settings of the current study are summarized in Figure 1. We first examined LPS-induced cardiomyocyte injuries. Electron microscopic analyses showed that massive cytoplasmic vacuolization was induced in the LPS-treated rat heart (Fig. 2c). In addition to the occurrence of cytoplasmic vacuoles, most of the LPS-treated rat myocardial mitochondria were swollen and severely damaged, and some mitochondria seemed to be surrounded by membranous structures (Fig. 2c). In the myocardium of LPS+CoPPIX-treated rat, some mitochondria seem to be degraded within the membranous structure (Fig. 2d), suggesting the autophagic elimination of damaged mitochondria.

### CoPPIX accelerates autophagy in response to LPS in rat heart

As we have shown previously that pretreatment with CoPPIX accelerates LPS-induced autophagy in the rat liver [20], we also evaluated the effects of CoPPIX on LPS-induced autophagy in the heart. As shown in Figure 3, activation of LC3, a marker of autophagy, peaked at 3 hours of treatment in the LPS alone group and at 1 hour in the LPS+CoPPIX group, suggesting that CoPPIX also accelerates LPS-induced autophagy in the heart. Degradation of the autophagy substrate p62 correlated well with the activation of LC3, suggesting an increase in autophagy flux. We next examined the levels of two transcription factors, NRF1 and TFAM, since the NRF1-TFAM axis links oxidative cellular stress to mitochondrial biogenesis and has been

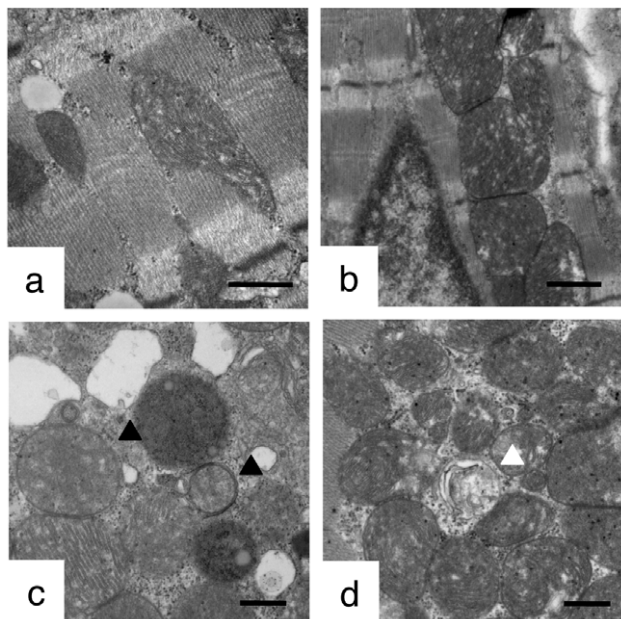


**Figure 2. Electron microscopic analysis of the LPS-treated rat heart.** Transmission electron micrographs of the rat heart treated with LPS (15 mg/kg, 3 h) with or without CoPPIX pretreatment (5 mg/kg, 24 h). Representative images in each group are shown: control (a), CoPPIX (b), LPS (c), LPS+CoPPIX (d). Bars, 500 nm. Black arrowheads indicate mitochondria swollen and/or surrounded by membranous structure. White arrowhead indicates mitochondria degraded within membranous structure.

doi:10.1371/journal.pone.0056526.g002

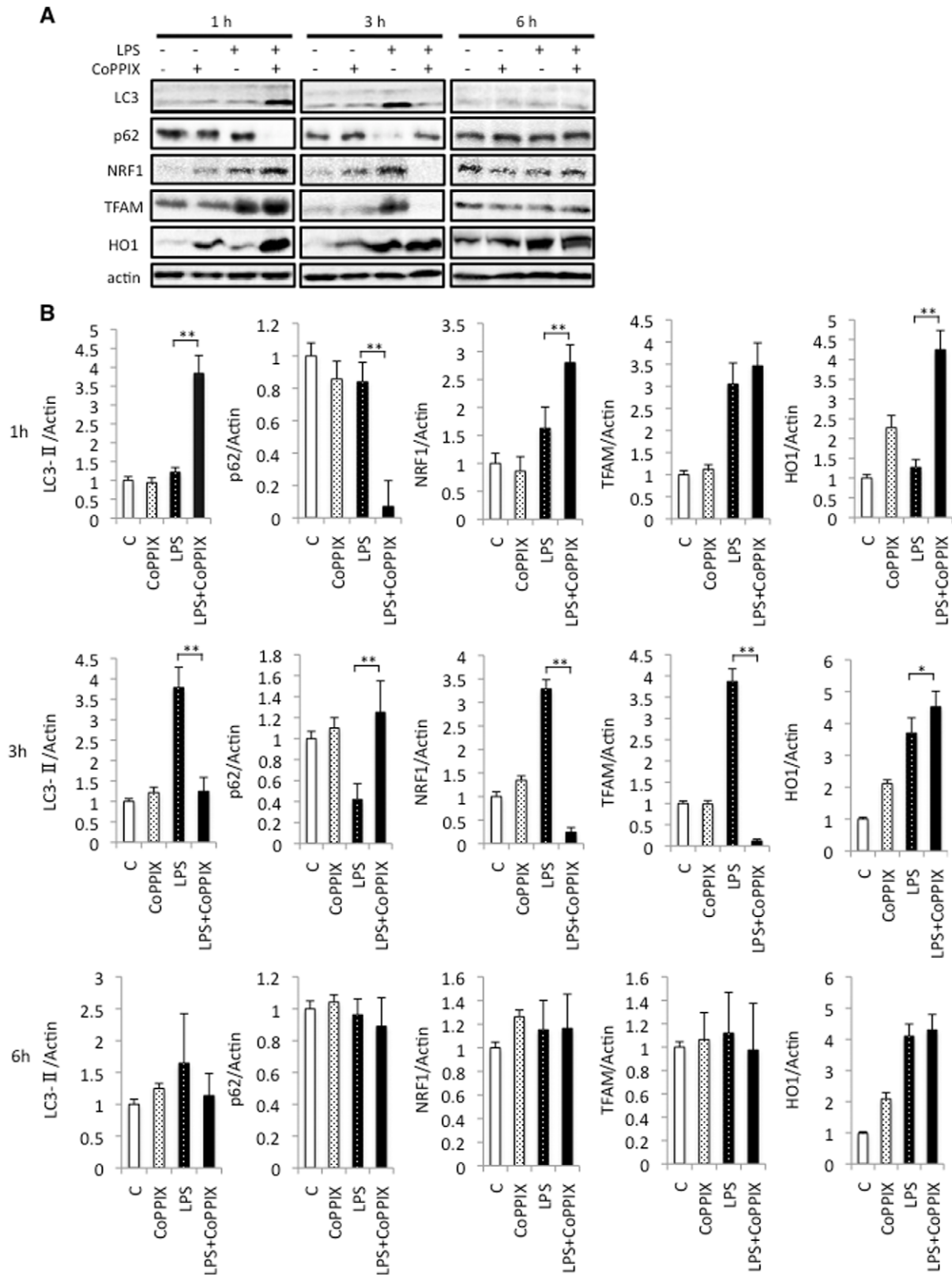


**Figure 3. Effects of CoPPIX on autophagy and mitochondrial biogenesis during LPS treatment in the heart.** A, Western blot analysis of the rat heart treated with LPS (15 mg/kg for 1, 3, and 6 h) with or without CoPPIX pretreatment (5 mg/kg, 24 h) to determine the levels of LC3-II, p62, NRF1, TFAM, and HO1. Actin was detected as a loading control. B, Ratios between LC3, p62, NRF1, TFAM, HO1, and actin determined using densitometry analysis. Each bar represents the mean  $\pm$  S.E. of four animals (\*\* $p < 0.01$ ; \* $p < 0.05$ ). Times indicated at the leftmost in the panel show the treatment times for LPS. doi:10.1371/journal.pone.0056526.g003

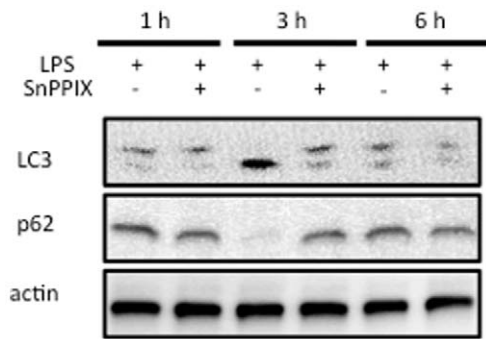


**Figure 4. Effects of SnPPIX on autophagy during LPS treatment in the heart.** Western blot analysis of the rat heart treated with LPS (15 mg/kg for 1, 3, and 6 h) with or without SnPPIX pretreatment (50 mg/kg, 24 h) to determine the levels of LC3-II and p62. Actin was detected as a loading control. Times indicated on the top of the panel show the treatment times for LPS.  
doi:10.1371/journal.pone.0056526.g004

shown to be activated during LPS treatment in the heart [7]. The NRF1-TFAM axis was found to be upregulated with faster kinetics in the LPS+CoPPIX groups than in the LPS alone group (Fig. 3A and B). Interestingly, NRF1 and TFAM are transiently depleted (3 hours after LPS) and then reformed (6 hours after LPS) in the hearts of the LPS+CoPPIX group (Fig. 3A and B). These results may indicate that the renewal of damaged mitochondria is more extensive in the LPS+CoPPIX group than in the LPS alone group. The expression of HO-1 was successfully induced in the heart by CoPPIX treatment (Fig. 3B), confirming the effect of this substance. LPS alone also induced HO-1 expression (Fig. 3B), consistent with previous reports. Increase of HO-1 in the heart of LPS+CoPPIX group was faster than that in LPS alone group, suggesting that CoPPIX should increase the cellular susceptibility to LPS (Fig. 3B).

#### SnPPIX suppresses autophagy in response to LPS in rat heart

To confirm the involvement of HO in the acceleration of autophagy in response to LPS, we also evaluated the effects of SnPPIX, HO inhibitor, on LPS-induced autophagy in the heart. As shown in Figure 4, neither LC3 activation nor p62 degradation was observed in the myocardium of SnPPIX+LPS-treated rat. We thus concluded that the effect of CoPPIX on autophagy is mediated through its effect on HO-1 induction.

#### CoPPIX enhances transient depletion and subsequent reformation of LAMP2 in response to LPS in the rat heart

We examined the status of the lysosomal marker proteins in our animal model. The level of LAMP1 showed the tendency to be upregulated in CoPPIX, LPS, and LPS+CoPPIX groups, but it seems to be difficult to deduce any meaning from the results. The level of LAMP2, which is involved in the elimination of autophagosome by lysosome, peaked at 3 hours of treatment in the LPS alone group and at 1 hour in the LPS+CoPPIX group (Fig. 5A and B). Like NRF1 and TFAM, LAMP2 is transiently depleted (3 hours after LPS treatment) and then reformed (6 hours after LPS treatment) in the hearts of the LPS+CoPPIX rats (Fig. 5A and B). The upregulation of TFEB was also observed in the LPS+CoPPIX hearts at 3 hours after LPS treatment (Fig. 5A and B).

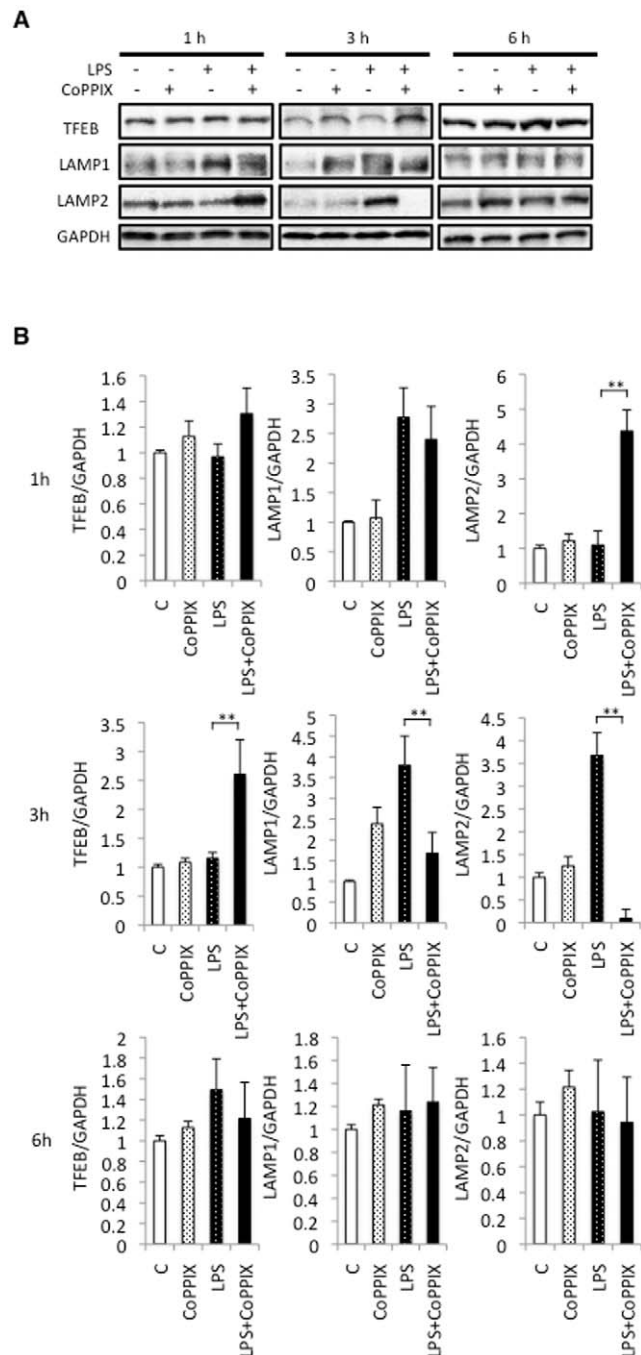


**Figure 5. Effects of CoPPIX on lysosome reformation during LPS treatment in the rat heart.** A, Western blot analysis of the rat heart treated with LPS (15 mg/kg for 1, 3, and 6 h) with or without CoPPIX pretreatment (5 mg/kg, 24 h) to determine the levels of TFEB, LAMP1, and LAMP2. GAPDH was detected as a loading control. B, Ratios between TFEB, LAMP1, LAMP2, and GAPDH determined using densitometry analysis. Each bar represents the mean  $\pm$  S.E. of four animals (\*\* $p < 0.01$ ). Times indicated at the leftmost side in the panel show the treatment times for LPS.  
doi:10.1371/journal.pone.0056526.g005

#### Immunohistochemical analysis of nuclear TFEB during LPS treatment

We next examined the cellular localization of TFEB, as it should be translocated from the cytoplasm to the nucleus upon

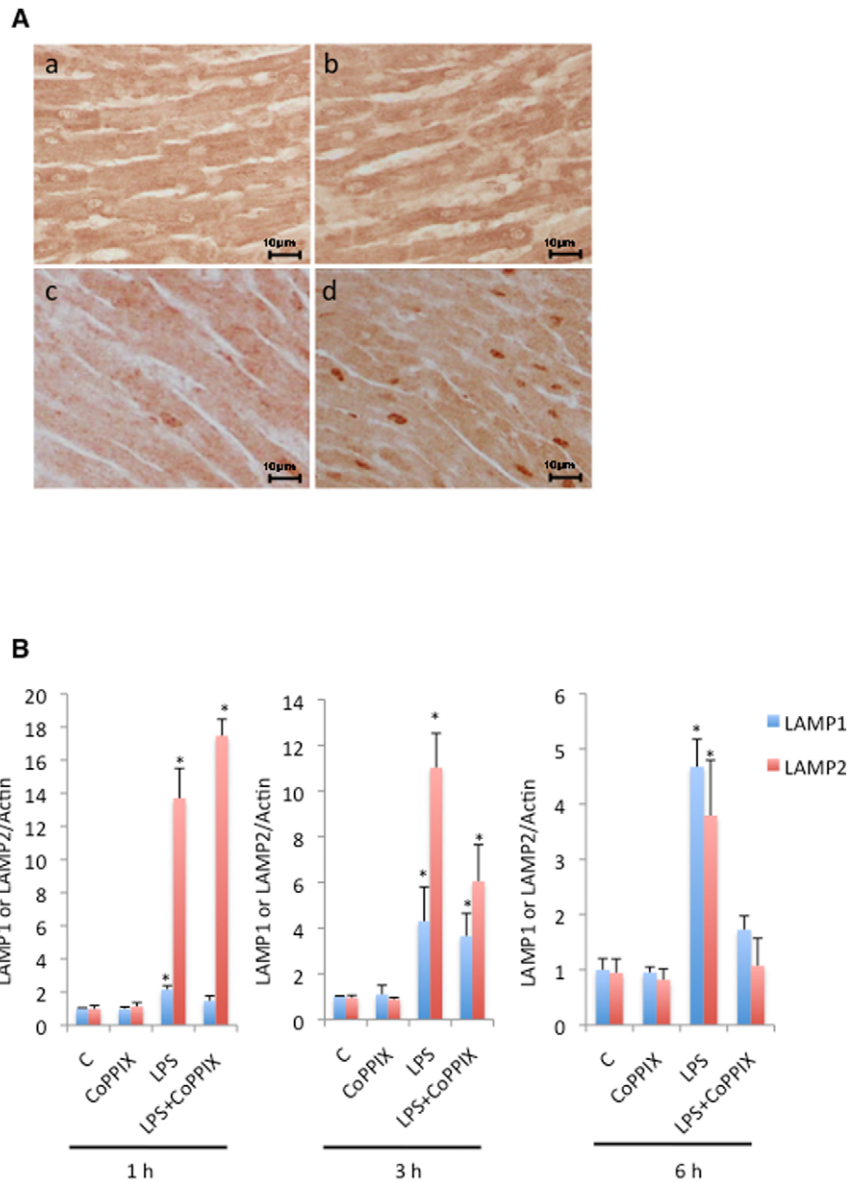


**Figure 6. Effects of CoPPIX on nuclear translocation and activation of TFEB during LPS treatment in the rat heart.** A, Immunohistochemical analysis of TFEB in the left ventricle of the rat heart at 3 h after LPS administration (15 mg/kg). Representative images in each group are shown: control (a), CoPPIX (b), LPS (c), LPS+CoPPIX (d). Bars, 5  $\mu$ m. B, RT-PCR analysis of the LAMP1 and LAMP2 levels in the heart of LPS-treated and control animals for 1, 3, and 6 h. Amplification of actin cDNA was performed and served as the internal control. Each bar represents the mean  $\pm$  S.E. of three animals (\* $p$ <0.05 vs. none). doi:10.1371/journal.pone.0056526.g006

activation. In contrast to the slight localization of TFEB in the nucleus of the rat hearts treated with LPS alone (Fig. 6A, c), strong nuclear localization was observed in the LPS+CoPPIX treated hearts (Fig. 6A, d). The mRNA levels of LAMP1 and LAMP2, both TFEB-target genes, were also upregulated in LPS and LPS+CoPPIX groups (Fig. 6B). It seems that the levels of LAMP2 mRNA peaked within 1 hour both in the LPS alone and LPS+CoPPIX groups (Fig. 6B). These data further confirm that TFEB is activated during LPS administration. CoPPIX pretreatment accelerates this activation.

#### Histological and serological evaluations of heart injuries caused by LPS-treatment in the rats

Histological comparisons of heart sections from LPS (24 hour)-treated septic rats with matching untreated controls revealed more prominent hemorrhaging following exposure to LPS (Fig. 7A). However, cell degeneration was not evident in either treatment group (Fig. 7A). In addition, CoPPIX treatment of the rats prevented heart damage (Fig. 7A). Oxidative stress events in the heart, as assessed by examining an oxidative stress marker 4-HNE adducts, during LPS treatment showed a higher number of 4-HNE-positive cells compared with the control (Fig. 7B, c). The CoPPIX-treated group, however, showed fewer 4-HNE-positive cells after LPS treatment (Fig. 7B, d). Hence, CoPPIX protects the

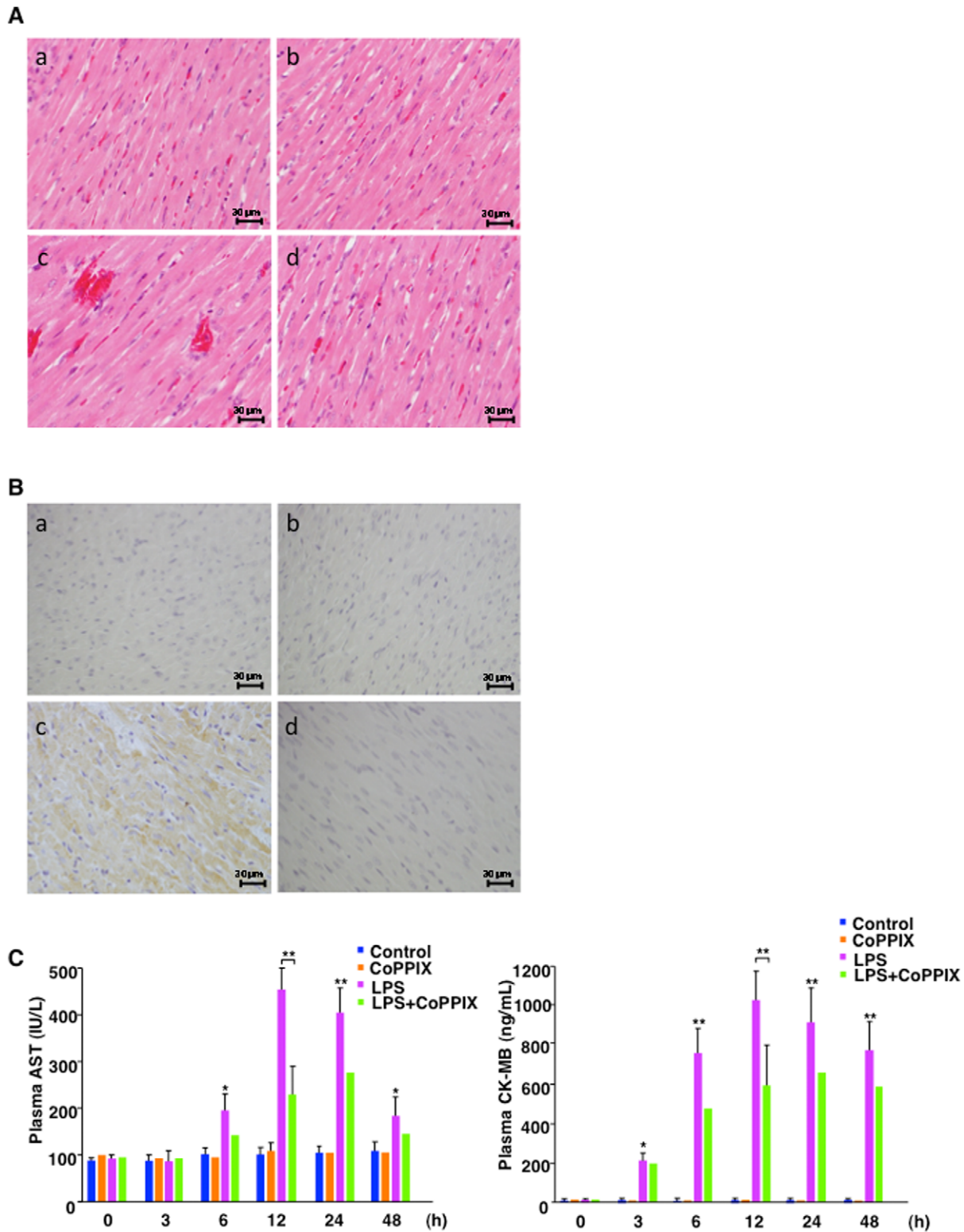


**Figure 7. Histological and serological analyses of heart injuries during LPS administration in rats.** A and B, Formalin-fixed and paraffin-embedded sections (3- $\mu$ m thickness) of rat heart tissues stained with H&E and with anti-4-HNE antibody. Representative H&E stains (A,  $\times 400$ ) and 4-HNE stains (B,  $\times 400$ ) in each group (four animals) are shown: control (a), CoPPIX (b), LPS (c), LPS+CoPPIX (d) for 24 h. Bars, 30  $\mu$ m. C, Plasma aspartate aminotransferase (AST, a) and creatine kinase-MB (CK-MB, b) concentrations for untreated control, CoPPIX (5 mg/kg, 24 h), LPS (15 mg/kg for indicated times), and LPS+CoPPIX groups. Values without error bars represent a single measurement while values with error bars represent mean  $\pm$  S.E. of four measurements (four animals). Statistical significance was determined between LPS and LPS+CoPPIX groups (12 h) or control and LPS groups (other time points) (\*\* $p < 0.01$ ; \* $p < 0.05$ ). doi:10.1371/journal.pone.0056526.g007

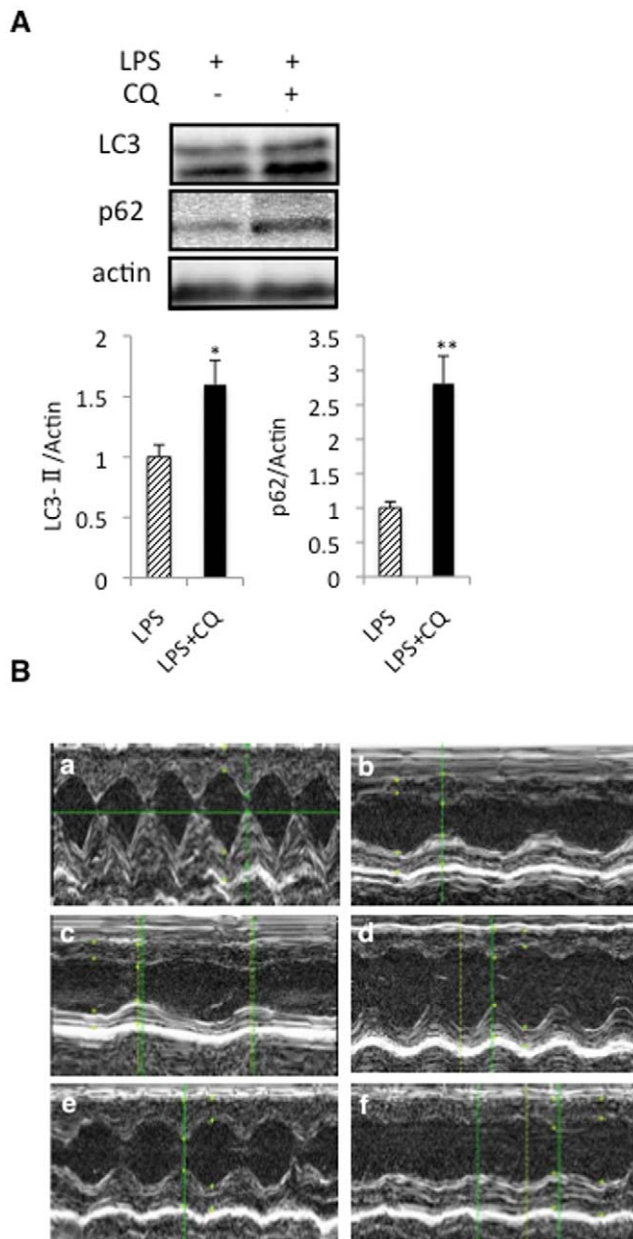


**Figure 8. Effects of CoPPIX on left ventricular function during LPS treatment in rats.** A, Western blot analysis of the rat heart with or without CQ treatment (20 mg/kg) with LPS treatment (15 mg/kg, 3 h) to determine the levels of LC3-II and p62. The ratios of LC3-II and p62 to actin were determined by densitometry analysis and are also represented. Each bar represents the mean  $\pm$  S.E. of four animals. \*\* $p < 0.01$ ; \* $p < 0.05$  vs. none. B, Representative echocardiographs in each group are shown: control (a), LPS for 3 h (b), LPS+CoPPIX for 3 h (c), LPS for 24 h (d), LPS+CoPPIX for 24 h (e), and LPS+CQ for 24 h (f). doi:10.1371/journal.pone.0056526.g008

heart against LPS-elicited oxidative stresses. These histological observations (Fig. 7 A and B) were found in all the samples (four rats/group) (data not shown). To further confirm the heart damage, we examined the plasma concentrations of serological markers of myocardial damage. We first examined plasma levels of aspartate aminotransferase (AST), which is mostly found in the liver and heart. AST was detected in the plasma after 6 hours and was found to be increased for at least 48 hours during LPS

treatment (Fig. 7C). To confirm the myocardial damage during LPS treatment, creatine kinase-MB (CK-MB), one of the most earliest and specific markers of heart damage was also examined. CK-MB was detected after 3 hours, earlier than AST, and remained to be elevated for at least 48 hours during LPS treatment (Fig. 7C). CoPPIX treatment reduced the plasma AST and CK-MB levels, confirming its protective effects against myocardial damage (Fig. 7C).

#### CoPPIX ameliorates, whereas CQ exacerbates, the reduced cardiac performance caused by LPS administration

Finally, we examined effects of CoPPIX, as well as of the lysosomal inhibitor CQ, on the reduced cardiac performance caused by LPS. As shown in Figure 8A, the LC3-II and p62 levels were significantly increased in the LPS+CQ group compared with the LPS alone group (Fig. 8A). Thus, CQ correctly induced lysosomal dysfunction and subsequent inhibition of autophagy flux in the rat heart. CQ also exacerbated the myocardial systolic dysfunction that was associated with LPS treatment, confirming the cardioprotective role of the autophagy/lysosome pathway in LPS-treated rats (Fig. 8B and Table 1). In contrast to the detrimental effect of CQ, pretreatment with CoPPIX tended to restore LPS-induced alterations in the myocardium (Fig. 8B and Table 1). Taken together, our current findings might indicate that CoPPIX ameliorates the left ventricular systolic dysfunction associated with LPS toxicity through enhancement of the autophagy/lysosome pathway.

#### Discussion

In our present study, we demonstrate the induction of autophagy in the heart during LPS administration. This process is accelerated by CoPPIX. In the heart of LPS+CoPPIX group, transient depletion and subsequent reformation of a lysosomal essential protein for autophagy, LAMP2, is observed. A master gene of lysosome biogenesis, TFEB, is also activated during LPS treatment, indicating that the TFEB activation and the subsequent reformation of lysosome are important for the protection of the heart against septic shock. Thus, our current results reveal for the first time the importance of TFEB activation in the LPS-treated heart. Results obtained in the current study are represented schematically in Figure 9.

TFEB, the somatic translocation of which is implicated in the renal carcinoma [23], is now implicated in lysosome biogenesis as well as autophagy induction [15,16]. Mitogen-activated protein kinase (MAPK) and mammalian target of rapamycin complex1 (mTORC1) are the protein/protein complex currently known to be responsible for the regulation of TFEB [15,16,24,25]. Thus, the relationship between mTORC1, MAPK, and TFEB activation during LPS insults should be examined in future studies. Interestingly, Palmieri et al., have observed that the genes involved in the recognition of pathogen associated molecular patterns, such as Toll-like receptor and Nod-like receptors, are upregulated in HeLa cells stably transfected with TFEB [26]. Therefore, the activation of TFEB might be also involved in the anti-inflammatory responses elicited by microbial pathogens, including those induced by LPS.

*LAMP1* and *LAMP2* are the genes dominantly regulated by TFEB [15,16]. In the process of chaperone-mediate autophagy, LAMP2A, a splicing variant of LAMP2, functions as a lysosomal receptor protein that receives the cytoplasmic proteins delivered to the lysosome [27]. LAMP2 also plays a pivotal role in macroautophagy [28]. A LAMP2 deficiency in the mouse results



**Table 1.** Echocardiographic parameters of left ventricular function were measured with LPS treatment (15 mg/kg) with or without CoPPiX (5 mg/kg) and CQ (20 mg/kg) for 3 and 24 h.

|              | Control  | LPS (3 h)  | LPS+CoPPiX (3 h) | LPS (24 h) | LPS+CoPPiX (24 h) | LPS+CQ (24 h)          |
|--------------|----------|------------|------------------|------------|-------------------|------------------------|
| HW/BW (mg/g) | 3.4±0.31 | 3.3±0.25   | 3.2±0.40         | 3.4±0.35   | 3.3±0.20          | 3.4±0.46               |
| LVDd (mm)    | 5.7±0.09 | 5.5±0.06   | 5.3±0.29         | 7.3±0.4**  | 6.8±0.3*          | 5.3±0.38 <sup>++</sup> |
| LVDs (mm)    | 3.2±0.06 | 3.23±0.12  | 3.4±0.15         | 3.1±0.15   | 3.5±0.17          | 3.25±0.20              |
| LVFS (%)     | 71.2±4.5 | 37.7±1.9** | 37.7±1.5**       | 37.5±3.9** | 48.4±3.8**        | 34.5±4.1 <sup>+</sup>  |
| EF (%)       | 96±1.7   | 75.1±2.2** | 75.8±1.8**       | 76.3±3.7** | 85.8±2.8*         | 72.3±4.5 <sup>+</sup>  |

Shown are heart-to-body weight ratio (HW/BW), left ventricular end-diastolic diameter (LVDd), left ventricular end-systolic diameter (LVDs), left ventricular fractional shortening (LVFS), and ejection fraction (EF). Each value represents the mean ± S.E. of four animals.

\*\* $p < 0.01$ ;

\* $p < 0.05$  vs. Control.

<sup>++</sup> $p < 0.01$ ;

<sup>+</sup> $p < 0.05$  vs. LPS (24 h).

doi:10.1371/journal.pone.0056526.t001

in the accumulation of autophagic vacuoles in many organs including the heart [22], suggesting its essential role in the clearance of autophagosomes in the heart. The phenotypes of the LAMP2-deficient mouse resemble human Danon disease [29]. Thus, a LAMP2 deficiency would result in incomplete autophagy in the heart and thus a rapid activation of TFEB and subsequent recovery of LAMP2 protein during LPS treatment should be a cardioprotective reaction necessary to complete the autophagy processes. Hsieh et al., have reported in this regard that the level of LAMP1 protein is gradually decreased in the left ventricle of the CLP (cecal ligation and puncture)-induced septic mouse [30]. Subsequent lysosome shortage resulted in an incomplete cytoprotective autophagy response [30]. Rapamycin treatment rescued the CLP-induced depression of cardiac performance through the resumption of autophagic flow [30]. Although we did not observe any significant decrease in LAMP1 protein levels within the treatment times tested in our current study, the transient LAMP2 depletion in LPS+CoPPiX-treated rat heart demonstrated in our present analyses represents further evidence for the increased

demand for lysosomes during septic insults in the heart. Very recently, the depletion of LAMP2 during hypoxia/reoxygenation in the mouse cardiomyocyte has been reported [31]. They also showed that adenovirus-mediated transfer of LAMP2 gene suppressed cell death during hypoxia/reoxygenation, suggesting the essential role of LAMP2 depletion and subsequent impairment of lysosomal function in the pathogenesis of ischemic heart [31].

Whereas high levels of CO inhibit mitochondrial cytochrome c oxidase activity, low levels of this compound afford cellular protection by generating low levels of reactive oxygen species (ROS) and causing a subsequent cellular adaptation that counteracts this stress event [32]. Detrimental responses due to the deficiency of HO-1 are rescued, at least in part, by the administration of CO [33]. CO has also been shown to be sufficient to induce autophagy in the mouse lung and in some cultured cells [34]. CO-releasing molecule (CO-RM) rescues mice from the CLP-induced lethal sepsis by activating mitochondrial biogenesis [35]. Although these findings suggest that CO might be sufficient to induce autophagy and mitochondrial biogenesis, we

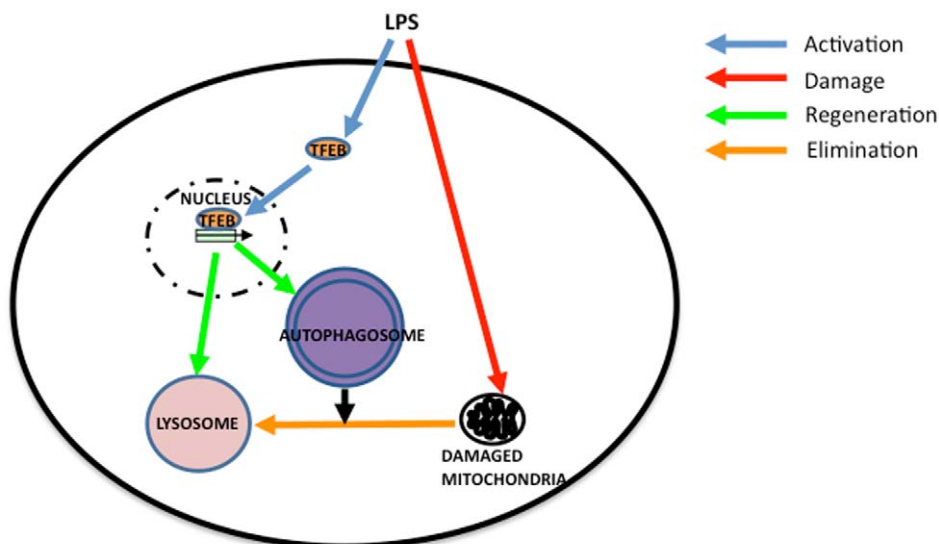


**Figure 9. Model of organelle turnover during LPS administration in rat heart.** TFEB pathway of autophagosomal and lysosomal biogenesis is activated in the heart to facilitate the elimination of damaged mitochondria during LPS administration. CoPPiX enhances the pathway and accelerates organelle turnover.

doi:10.1371/journal.pone.0056526.g009

could not observe any augmentation of these processes or lysosome reformation in our CoPPIX alone treated rats (Figs. 3 and 5). Therefore, cellular reactions caused by LPS, such as ROS formation, are likely to be essential for these processes i.e. CoPPIX play roles in the augmentation/acceleration of these pathways during LPS treatment.

As shown in Figure 3A, induction of HO-1 in response to LPS was much faster in the LPS+CoPPIX group than in the LPS group. We do not know exact reason why HO-1 is induced more rapidly in the heart of LPS+CoPPIX group than LPS group. As CoPPIX has been shown to induce HO-1 expression, at least in parts, through decreasing the degradation of HO-1-inducing transcription factor Nrf2 [36]. Thus, fast induction of HO-1 during subsequent treatment with LPS in LPS+CoPPIX group might be a result of the higher availability of Nrf2. In accordance with the idea, we observed increase of Nrf2 protein in the heart of CoPPIX group (data not shown). In the current study, cardioprotective effect of CoPPIX was evaluated both histologically (Fig. 7A and B) and serologically (Fig. 7C). Besides heart, CK-MB is also found in other organs such as skeletal muscle [37]. Due to the limited tissue specificity of serological biomarkers, we also evaluated heart damage histologically. Oxidative stress by LPS and its amelioration by CoPPIX were proved in the heart (Fig. 7B). Although CoPPIX is considered to be the most potent inducer of

HO among the metalloporphyrins [19], deleterious side effects have been reported for this compound [38,39,40]. Schmidt et al. have shown that isoflurane, an anesthetic medicine frequently used in the current clinical practice, is a potent inducer of HO-1 in the liver [40,41]. Thus, isoflurane could potentially serve as an alternative for CoPPIX, although its effect on the heart would need to be examined. It should also be noted that injuries during LPS-induced endotoxin shock in the rat lung and liver are ameliorated by trehalose [42]. Trehalose is a potent inducer of autophagy [43] and is an activator of TFEB [15]. Hence, the beneficial effects of trehalose on septic insults might arise not only from its anti-oxidative effects but also through TFEB activation.

In conclusion, TFEB activation and subsequent lysosome reformation during septic shock in the heart is presented. Acceleration of this possible cardioprotective response by HO/CoPPIX may have novel therapeutic implications for critically ill patients with sepsis.

## Author Contributions

Conceived and designed the experiments: K. Unuma TA K. Uemura. Performed the experiments: K. Unuma TA TF. Analyzed the data: K. Unuma TA K. Uemura. Contributed reagents/materials/analysis tools: KY. Wrote the paper: K. Unuma TA K. Uemura.

## References

- Lin WJ, Yeh WC (2005) Implication of Toll-like receptor and tumor necrosis factor alpha signaling in septic shock. *Shock* 24: 206–209.
- Boyd JH, Mathur S, Wang Y, Bateman RM, Walley KR (2006) Toll-like receptor stimulation in cardiomyocytes decreases contractility and initiates an NF-kappaB dependent inflammatory response. *Cardiovasc Res* 72: 384–393.
- Avlas O, Fallach R, Shainberg A, Porat E, Hochhauser E (2011) Toll-like receptor 4 stimulation initiates an inflammatory response that decreases cardiomyocyte contractility. *Antioxid Redox Signal* 15: 1895–1909.
- Andrades M, Ritter C, de Oliveira MR, Streck EL, Fonseca Moreira JC, et al. (2011) Antioxidant treatment reverses organ failure in rat model of sepsis: role of antioxidant enzymes imbalance, neutrophil infiltration, and oxidative stress. *J Surg Res* 167: e307–313.
- Dare AJ, Phillips AR, Hickey AJ, Mittal A, Loveday B, et al. (2009) A systematic review of experimental treatments for mitochondrial dysfunction in sepsis and multiple organ dysfunction syndrome. *Free Radic Biol Med* 47: 1517–1525.
- Gottlieb RA, Carreira RS (2010) Autophagy in health and disease. 5. Mitophagy as a way of life. *Am J Physiol Cell Physiol* 299: C203–210.
- Suliman HB, Carraway MS, Tatro LG, Piantadosi CA (2007) A new activating role for CO in cardiac mitochondrial biogenesis. *J Cell Sci* 120: 299–308.
- Piantadosi CA, Carraway MS, Babiker A, Suliman HB (2008) Heme oxygenase-1 regulates cardiac mitochondrial biogenesis via Nrf2-mediated transcriptional control of nuclear respiratory factor-1. *Circ Res* 103: 1232–1240.
- Yuan H, Perry CN, Huang C, Iwai-Kanai E, Carreira RS, et al. (2009) LPS-induced autophagy is mediated by oxidative signaling in cardiomyocytes and is associated with cytoprotection. *Am J Physiol Heart Circ Physiol* 296: H470–479.
- Hickson-Bick DL, Jones C, Bujala LM (2008) Stimulation of mitochondrial biogenesis and autophagy by lipopolysaccharide in the neonatal rat cardiomyocyte protects against programmed cell death. *J Mol Cell Cardiol* 44: 411–418.
- Suliman HB, Sweeney TE, Withers CM, Piantadosi CA (2010) Co-regulation of nuclear respiratory factor-1 by NFkappaB and CREB links LPS-induced inflammation to mitochondrial biogenesis. *J Cell Sci* 123: 2565–2575.
- Yu L, McPhee CK, Zheng L, Mardones GA, Rong Y, et al. (2010) Termination of autophagy and reformation of lysosomes regulated by mTOR. *Nature* 465: 942–946.
- Dehay B, Bove J, Rodriguez-Muela N, Perier C, Recasens A, et al. (2010) Pathogenic lysosomal depletion in Parkinson's disease. *J Neurosci* 30: 12535–12544.
- Fortunato F, Burgers H, Bergmann F, Rieger P, Buchler MW, et al. (2009) Impaired autolysosome formation correlates with Lamp-2 depletion: role of apoptosis, autophagy, and necrosis in pancreatitis. *Gastroenterology* 137: 350–360. doi: 10.1053/j.gastro.2009.05.035
- Sardiello M, Palmieri M, di Ronza A, Medina DL, Valenza M, et al. (2009) A gene network regulating lysosomal biogenesis and function. *Science* 325: 473–477.
- Settembre C, Di Malta C, Polito VA, Garcia Arencibia M, Vetrini F, et al. (2011) TFEB links autophagy to lysosomal biogenesis. *Science* 332: 1429–1433.
- Ma X, Godar RJ, Liu H, Diwan A (2012) Enhancing lysosome biogenesis attenuates BNIP3-induced cardiomyocyte death. *Autophagy* 8: 100–110.
- Ryter SW, Alam J, Choi AM (2006) Heme oxygenase-1/carbon monoxide: from basic science to therapeutic applications. *Physiol Rev* 86: 583–650.
- Shan Y, Pepe J, Lu TH, Elbirt KK, Lambrecht RW, et al. (2000) Induction of the heme oxygenase-1 gene by metalloporphyrins. *Arch Biochem Biophys* 380: 219–227.
- Unuma K, Aki T, Matsuda S, Funakoshi T, Yoshida KI, et al. (2012) Inducer of heme oxygenase-1 cobalt protoporphyrin accelerates autophagy and suppresses oxidative damages during lipopolysaccharide treatment in rat liver. *Hepatol Res* 42: 100–108.
- Carchman EH, Rao J, Loughran PA, Rosengart MR, Zuckerbraun BS (2011) Heme oxygenase-1-mediated autophagy protects against hepatocyte cell death and hepatic injury from infection/sepsis in mice. *Hepatology* 53: 2053–2062.
- Tanaka Y, Guhde G, Suter A, Eskelinen EL, Hartmann D, et al. (2000) Accumulation of autophagic vacuoles and cardiomyopathy in LAMP-2-deficient mice. *Nature* 406: 902–906.
- Srigley JR, Delahunt B (2009) Uncommon and recently described renal carcinomas. *Mod Pathol* 22 Suppl 2: S2–S23.
- Pena-Llopis S, Vega-Rubin-de-Celis S, Schwartz JC, Wolff NC, Tran TA, et al. (2011) Regulation of TFEB and V-ATPases by mTORC1. *EMBO J* 30: 3242–3258.
- Settembre C, Zoncu R, Medina DL, Vetrini F, Erdin S, et al. (2012) A lysosome-to-nucleus signalling mechanism senses and regulates the lysosome via mTOR and TFEB. *EMBO J* 31: 1095–1108.
- Palmieri M, Impey S, Kang H, di Ronza A, Pelz C, et al. (2011) Characterization of the CLEAR network reveals an integrated control of cellular clearance pathways. *Hum Mol Genet* 20: 3852–3866.
- Cuervo AM, Dice JF (1996) A receptor for the selective uptake and degradation of proteins by lysosomes. *Science* 273: 501–503.
- Ruivo R, Anne C, Sagne C, Gasnier B (2009) Molecular and cellular basis of lysosomal transmembrane protein dysfunction. *Biochim Biophys Acta* 1793: 636–649.
- Nishino I, Fu J, Tanji K, Yamada T, Shimojo S, et al. (2000) Primary LAMP-2 deficiency causes X-linked vacuolar cardiomyopathy and myopathy (Danon disease). *Nature* 406: 906–910.
- Hsieh CH, Pai PY, Hsueh HW, Yuan SS, Hsieh YC (2011) Complete induction of autophagy is essential for cardioprotection in sepsis. *Ann Surg* 253: 1190–1200.
- Ma X, Liu H, Foyil SR, Godar RJ, Weinheimer CJ, et al. (2012) Impaired Autophagosome Clearance Contributes to Cardiomyocyte Death in Ischemia-Reperfusion Injury. *Circulation* 126: 1000–1009.
- Zuckerbraun BS, Chin BY, Bilban M, d'Avila JC, Rao J, et al. (2007) Carbon monoxide signals via inhibition of cytochrome c oxidase and generation of mitochondrial reactive oxygen species. *FASEB J* 21: 1099–1106.
- Chen B, Guo L, Fan C, Bolisetty S, Joseph R, et al. (2009) Carbon monoxide rescues heme oxygenase-1-deficient mice from arterial thrombosis in allogeneic aortic transplantation. *Am J Pathol* 175: 422–429.
- Lee SJ, Ryter SW, Xu JF, Nakahira K, Kim HP, et al. (2011) Carbon monoxide activates autophagy via mitochondrial reactive oxygen species formation. *Am J Respir Cell Mol Biol* 45: 867–873.

35. Lancel S, Hassoun SM, Favory R, Decoster B, Motterlini R, et al. (2009) Carbon monoxide rescues mice from lethal sepsis by supporting mitochondrial energetic metabolism and activating mitochondrial biogenesis. *J Pharmacol Exp Ther* 329: 641–648.
36. Shan Y, Lambrecht RW, Donohue SE, Bonkovsky HL (2006) Role of Bach1 and Nrf2 in up-regulation of the heme oxygenase-1 gene by cobalt protoporphyrin. *FASEB J* 20: 2651–2653.
37. O'Brien PJ (2008) Cardiac troponin is the most effective translational safety biomarker for myocardial injury in cardiotoxicity. *Toxicology* 245: 206–218.
38. Galbraith RA, Kappas A (1989) Regulation of food intake and body weight by cobalt porphyrins in animals. *Proc Natl Acad Sci U S A* 86: 7653–7657.
39. Smith TJ, Drummond GS, Kappas A (1987) Cobalt-protoporphyrin suppresses thyroid and testicular hormone concentrations in rat serum: a novel action of this synthetic heme analogue. *Pharmacology* 34: 9–16.
40. Schmidt R, Tritschler E, Hoetzel A, Loop T, Humar M, et al. (2007) Heme oxygenase-1 induction by the clinically used anesthetic isoflurane protects rat livers from ischemia/reperfusion injury. *Ann Surg* 245: 931–942.
41. Schmidt R, Hoetzel A, Baechle T, Loop T, Humar M, et al. (2004) Isoflurane pretreatment lowers portal venous resistance by increasing hepatic heme oxygenase activity in the rat liver in vivo. *J Hepatol* 41: 706–713.
42. Minutoli L, Altavilla D, Bitto A, Polito F, Bellocco E, et al. (2008) Trehalose: a biophysics approach to modulate the inflammatory response during endotoxic shock. *Eur J Pharmacol* 589: 272–280.
43. Sarkar S, Davies JE, Huang Z, Tunnacliffe A, Rubinsztein DC (2007) Trehalose, a novel mTOR-independent autophagy enhancer, accelerates the clearance of mutant huntingtin and alpha-synuclein. *J Biol Chem* 282: 5641–5652.